a reprint from Applied Optics

Practical example of the correction of Fourier-transform spectra for detector nonlinearity

M. C. Abrams, G. C. Toon, and R. A. Schindler

HgCdTe photoconductive detectors can display a nonlinear response when illuminated. In interferometric applications, this behavior must be accounted for in the data transformation process to avoid errors in the measurement of the spectral distribution of the incident radiation. A model for the distortion of the interferogram is proposed and applied to solar observations made by the Atmospheric Trace Molecule Spectroscopy (ATMOS) Fourier-transform spectrometer during orbital sunrise and sunset from the Space Shuttle. Empirical estimation of the dc current level is necessary for this instrument, and satisfactory nonlinearity correction is obtained for several of the primary ATMOS optical filters. For ATMOS broadband optical filters that cover more than one half the alias bandwidth, the model is inadequate because of the presence of antialiasing electronic filters within the instrument, and it is necessary to resort to estimation and subtraction of the residual baseline offset. In either case the remaining baseline offsets are typically smaller than 1%, which is satisfactory, although offset remains a significant systematic source of error in the estimation of the abundance of telluric and solar constituents from the spectra.

Introduction

In an ideal photometric detector the measured signal is linearly proportional to the incident flux of radiation; in practice, photoconductive infrared mercury cadmium telluride (HgCdTe) detectors can display a nonlinear response when illuminated. Bartoli *et al.*[1] have demonstrated that for photon fluxes in excess of 10^{19} photons cm^{-2} s^{-1} the minority lifetime in photoconductive HgCdTe is linearly proportional not to the photon flux Φ but rather to $\Phi^{-2/3}$, producing an electrical conductivity proportional to the cube root of the photon flux. Kinch and Borrello[2] and Borrello *et al.*[3] have demonstrated that this behavior is consistent with Auger recombination of carriers within the detector. Schindler[4] has further demonstrated that series resistance can cause the measurement to be nonlinear regardless of the illumination of the detector. For a voltage-biased photoconductive detector, this causes the voltage output

$$\Delta V = \frac{K_1\Phi}{(1 + K_2\Phi)} \qquad (1)$$

in response to a photon flux Φ, where K_1 and K_2 are constants that depend on the optical throughput and the circuit parameters. Although it is generally the case that $K_1 \gg K_2$, the measured signal is not a linear representation of the incident photon flux, and the signal must be corrected in some fashion to represent the distribution of radiation properly.

In interferometric systems, linearity is important because of the large variation in photon flux experienced by the detector as the optical path difference passes through zero. These variations are particularly severe in solar observations, where the source fluxes greatly exceed the instrumental background. If the central fringe amplitude is affected by nonlinearity in the detection and sampling process, then the quality of the resulting spectrum will be greatly reduced by the distortion of the continuum; the zero level may be offset within the spectral bandpass, and out-of-band spectral artifacts may be created in the spectrum, both of which introduce systematic errors in the measurement of the abundance of telluric and solar constituents from such a spectrum.

The typical solution to the introduction of errors is to restrict the photon flux, either by restricting the field of view, the aperture, or the spectral range, or all three. Unfortunately this degrades the signal-to-noise ratio and hence the measurement capability. An alternative solution is to develop a model of the detector–preamplifier response that can be used to

The authors are with the Jet Propulsion Laboratory, California Institute of Technology, Pasadena, California 91109.

Received 25 August 1993; revised manuscript received 11 April 1994.

0003-6935/94/276307-08$06.00/0.

correct the measured interferogram before transformation. A nonlinearity-correction strategy that successfully reduces the in-band intensity offsets from 1–10% to less than 1% is proposed.

We propose a model based on the expected behavior of the detector and have expanded this concept in a power series expansion in the form of multiple correlations of the interferogram. In practice, interferograms can be substantially corrected to remove the detector and electronic nonlinearity; however, the aliasing of nonlinear harmonics places a restriction on the limits of the spectral bandpass that can be adequately corrected. We examine these problems in the light of the practical requirements provided by the Atmospheric Trace Model Spectroscopy (ATMOS) interferometer, which is flown aboard a Space Shuttle on a near annual basis to study the Earth's atmosphere.

The implications of nonlinear detector response in absorption spectroscopy have been examined in several previous papers. Chase[5] demonstrated a convenient method of detecting and removing the nonlinearity based on an autocorrelation of the observed spectrum. The interaction between phase correction and nonlinearity correction was illustrated with synthetic data. Practical application of the method with experimental data was not included, and in particular the issue of aliasing was not addressed. Guelachvili[6] developed a new method for removing nonlinearity from two-output Fourier-transform spectrometers by combining the modulated outputs, which have the same amplitudes and opposite phases, in a manner in which the nonlinear signal cancels itself out. This would be a highly desirable solution but is not applicable to an existing single detector instrument. Schindler[4] proposed a nonlinearity-correction circuit for photoconductive detectors that compensated for series resistance. Carter *et al.*[7] illustrated a reduced nonlinear response from HgCdTe detectors by changing the detector biasing from constant current to constant voltage, which significantly alters the detector response but does not further address the fundamental problem for constant-current-biased detectors.

ATMOS Fourier-Transform Spectrometer

The ATMOS instrument is a high-resolution Fourier-transform spectrometer that measures solar spectra from the Space Shuttle during orbital sunset and sunrise. From the atmospheric absorptions in these spectra the structure and composition of the middle and upper atmosphere are derived.[8] Within the ATMOS instrument, interferometrically modulated solar radiation is focused onto a HgCdTe photoconductor (2–16 μm), with mean flux levels between 0.2×10^{19} and 1.2×10^{19} photons $cm^{-2}\ s^{-1}$, depending on the field of view and the optical bandpass filter selected. These spectra display spectral artifacts that are indicative of nonlinear distortion of the interferogram in the detection and sampling process. Nearly all the spectra have large spectral features between zero- and the low-frequency detector cutoff at 650 cm^{-1}, which Chase[5] has demonstrated are typical of spectra obtained with poor detector linearity and may be described in terms of the autocorrelation of the intended spectrum. Spectral artifacts at frequencies larger than the high-frequency cutoff of the optical filter and in-band zero offsets beneath saturated spectral features are indicative of a higher-order nonlinear response in the detector and sampling process.

In-band spectral offsets introduce systematic errors in the measured equivalent width of absorption lines. Figure 1 compares the fractional error in the retrieved concentration (nominally the equivalent width) of a CO_2 line at 957.8 cm^{1} retrieved for three spectra with air masses corresponding to approximately 10, 20, and 50% central absorption depths. As the zero-level intensity offset is increased from 1 to 10%, the fractional error increases for each of the lines in a near-linear fashion. However, the gradient increases from near unity for weak lines to 2 or 3 for strong lines. Thus the bias introduced by strong lines will be greater than the bias introduced by weak lines.

For ground-based or high-air-mass spectra exhibiting saturated absorption features it is possible to correct empirically for the offset of the zero baseline, but for upper atmospheric and solar spectra such methods are ineffective because none of the absorption features is saturated and there is no way to estimate zero offsets accurately within the spectral bandpass of the filter. Out-of-band spectral artifacts are observed in all spectra and may affect the assay of

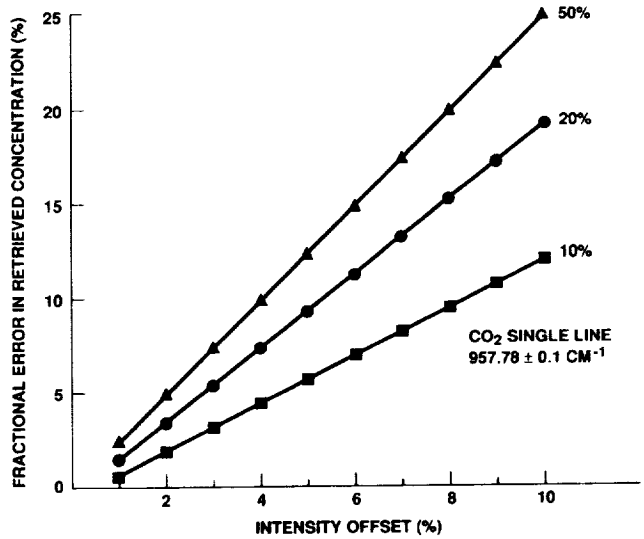

Fig. 1. Fractional error in retrieved concentration as a function of the zero-level intensity offset for a well-resolved and isolated CO_2 line at 957.78 cm^{-1} observed at air masses corresponding to weak (10%), intermediate (20%), and strong (50%) absorptions in the transmission spectra. The error is a near-linear function of the intensity offset. Intensity offsets between 1 and 10% are commonly observed and need to be corrected to the 1% level to minimize any systematic biasing because of residual zero-level intensity offsets.

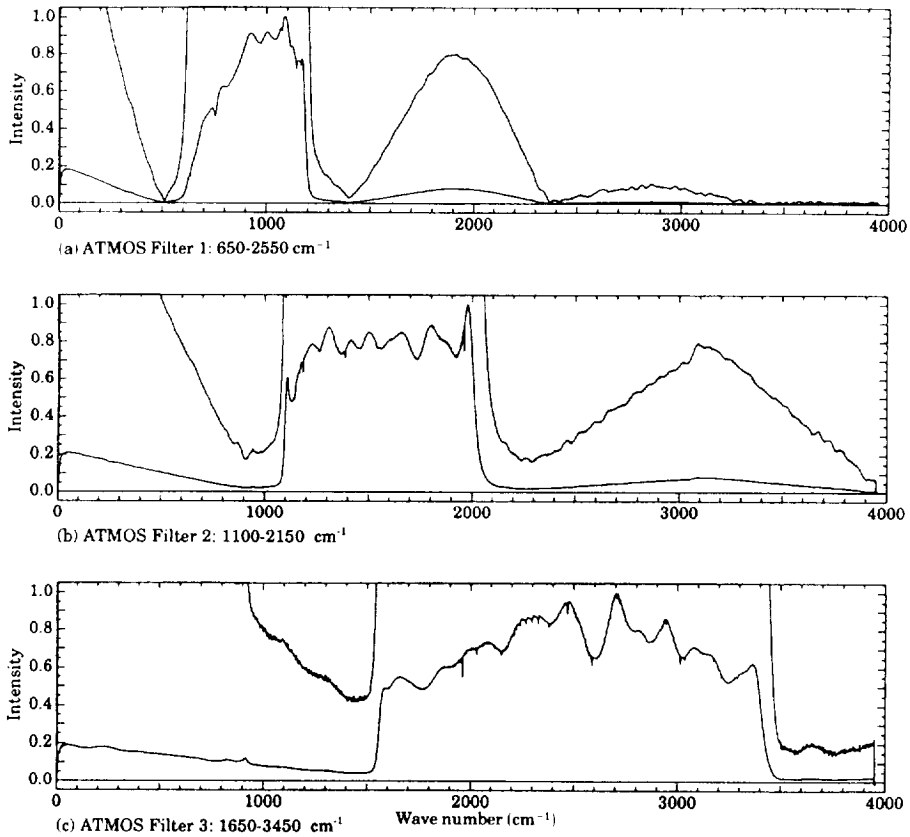

Fig. 2. Uncorrected low-resolution solar spectra obtained with ATMOS filters 1, 2, and 3. Each frame contains two traces, with the upper trace enlarged in the vertical by a factor of 10 to enhance the out-of-band spectral artifacts.

atmospheric or solar constituents by altering the absolute photometric distribution. If the optical bandpass includes the upper half of the spectral alias, the nonlinear response of the detector will be aliased, or folded back, into the optical bandpass and introduce additional intensity offsets.

Figure 2 illustrates high-Sun spectra obtained with three of the ATMOS optical filters covering portions of the 0–3950 cm^{-1} first-order alias bandwidth. The filters were selected to cover the bandpass between the 650-cm^{-1} cutoff of the HgCdTe detector and the alias cutoff at 4000 cm^{-1} with the purpose of preventing the short-wavelength photon noise from degrading the weaker long-wavelength signals. Filter 1 covers the spectral region between 650 and 1150 cm^{-1}, filter 2 covers the region between 950 and 2050 cm^{-1} and filter 3 covers the region between 1550 and 3450 cm^{-1}. In terms of the alias bandwidth, the filters cover approximately one eighth, one quarter, and one half the alias bandwidth respectively, with filter 3 lying mostly in the upper half of the alias. Several features are significant and noteworthy: (a) the spectra contain a large low-frequency feature that resembles a triangle, (b) the filter 1 and filter 2 spectra contain spectral artifacts at twice the respective central frequencies that are a significant component of the total spectral flux (area beneath the curve), (c) the filter 1 spectrum contains a spectral artifact at 3 times the central frequency of that filter, (d) as the filter width is increased the width of the artifacts increases as well, and (e) in the filter 3 spectrum the high-frequency spectral artifacts are aliased into the spectral bandpass of the filter.

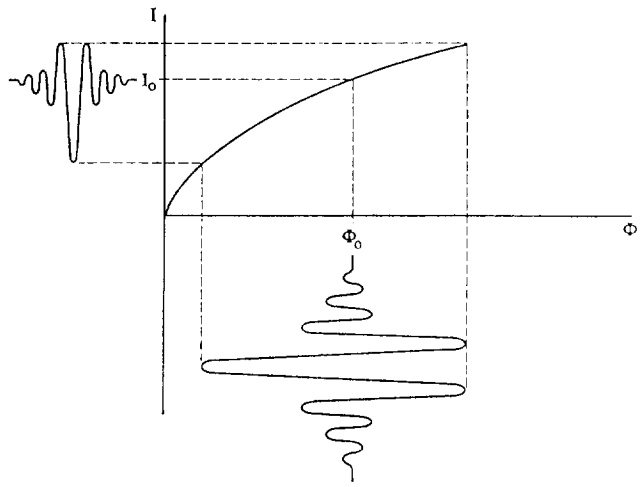

Fig. 3. Hypothetical detector-response curve exhibiting nonlinearity. The horizontal axis represents the absolute magnitude of the photon flux and the vertical axis represents the measured dc signal. The stylized representations of the interferograms illustrate the relative distortion of the central fringe compared with the rest of the interferogram under the assumption of 70% modulation efficiency.

Methods

We propose a correction strategy based on a model of nonlinearity resulting from a reduction in the photoresponsivity of the detector because of Auger recombination, which defines a particular shape for the nonlinear response curve of the detector. Practically, the model only provides a plausibility argument for a curve with which the actual measured interferograms can be manipulated. Additional considerations such as saturation effects would also produce nonlinear response curves, and in practice we cannot rule out the possibility that the correction strategy proposed does not also include empirical corrections for non-detector-signal distortions. Unfortunately we are constrained to working with a filtered and sampled measurement of the true detector photoconductivity and not the actual conductance produced in the detector.

A hypothetical detector-response curve exhibiting detector nonlinearity is illustrated in Fig. 3. The abscissa represents the absolute magnitude of the photon flux, and the ordinate represents the dc detector current. Beneath the x axis is a representation of an interferogram; under ideal conditions the flux would range from 0 to twice the dc flux level Φ_0, but in practice the modulation efficiency is less than unity, as suggested by the curve. To the left of the y axis is a representation of the measured interferogram after distortion by the nonlinear detector.

Let us assume that the measured signal is proportional to the cube root of the flux,

$$I(x) = a\Phi(x)^{1/3} \tag{2}$$

and consequently the dc signal is $I_0 = a\Phi_0^{1/3}$, where a is an unknown constant of proportionality and Φ_0 is the unmodulated (dc) solar intensity. In an ac-coupled preamplifier the measured quantity is $I_{AC} = I - I_0$, from which we desired to recover the true representation of the signal, which we may estimate as

$$[I(x) - I_0]_{TRUE} = [\Phi(x) - \Phi_0(x)] \Big/ \left[\frac{\partial\Phi(x)}{\partial I(x)}\right]_{I_0}. \tag{3}$$

Because $\Phi - \Phi_0 = (I/a)^3 - (I_0/a)^3$ and $(\partial\Phi/\partial I)_{I_0} = 3I_0^2/a^3$, the renormalized interferogram is

$$[I(x) - I_0]_{TRUE} = I_{AC}(x)\left\{1 + \frac{I_{AC}(x)}{I_0} + \frac{1}{3}\left[\frac{I_{AC}(x)}{I_0}\right]^2\right\}. \tag{4}$$

Immediately one may observe that away from the central fringe $I_{AC} \ll I_0$, and the expression reduces to I_{AC}, which simply reflects that fact that the flux variation about the dc level is small far from the central fringe and consequently the nonlinear distor-

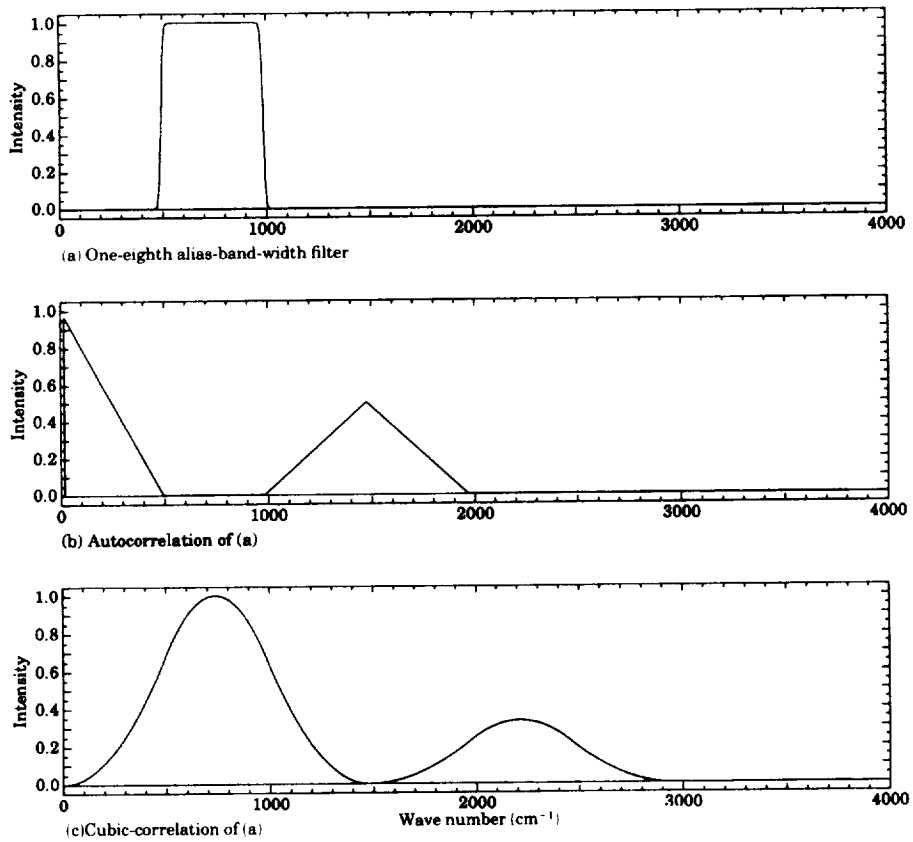

Fig. 4. (a) One-eighth alias-bandwidth model of ATMOS filter 1, (b) autocorrelation of (a), (c) cubic correlation of (a). Notice the spectral artifacts near zero frequency and twice the central frequency in (b) and the feature at 3 times the central frequency of the filter in (c). Additionally, the largest cubic-correlation term lies within the bandpass of the filter.

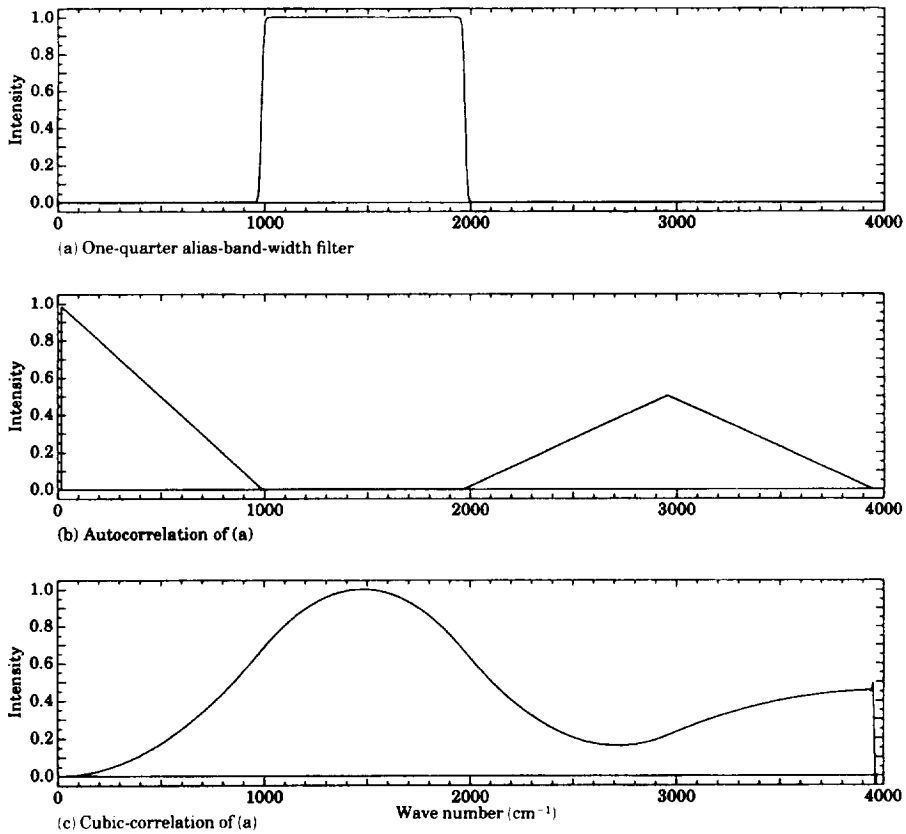

Fig. 5. (a) One-quarter alias-bandwidth model of ATMOS filter 2, (b) autocorrelation of (a), (c) cubic correlation of (a). Notice the spectral artifacts near zero frequency and twice the central frequency in (b). The sum frequency artifact in (b) occupies most of the upper half of the alias bandwidth. Aliasing is apparent in (c) as the cube frequency artifact is centered at a frequency above the alias cutoff and the hence folded back into the spectrum.

tion is minimal. The only unknown in the expression for the corrected interferogram is the dc signal I_0, because the constant of proportionality a cancels out.

Such a model will be recognized as being closely related to a generalized power series expansion of the interferogram of the form

$$I_{\mathrm{OBS}}(x) = I(x) + \alpha I^2(x) + \beta I^3(x) \ldots, \qquad (5)$$

where x is the path difference with respect to the location of the central fringe. A Fourier transform of such an interferogram will yield a spectrum

$$\begin{aligned} S_{\mathrm{OBS}}(\sigma) &= \int_{-\infty}^{+\infty} I_{\mathrm{OBS}}(x)\exp(-i2\pi\sigma x)\mathrm{d}x \\ &= \int_{-\infty}^{+\infty} I(x)\exp(-i2\pi\sigma x)\mathrm{d}x \\ &\quad + \alpha \int_{-\infty}^{+\infty} I^2(x)\exp(-i2\pi\sigma x)\mathrm{d}x \\ &\quad + \beta \int_{-\infty}^{+\infty} I^3(x)\exp(-i2\pi\sigma x)\mathrm{d}x + \cdots, \end{aligned} \qquad (6)$$

in which the desired spectrum, as a function of frequency σ, is the transform of the first term, and the higher-order terms are correlation harmonics, beginning with the autocorrelation

$$S(\sigma) * S(\sigma) = \int_{-\infty}^{+\infty} I^2(x)\exp(-i2\pi\sigma x)\mathrm{d}x. \qquad (7)$$

When such a model is applied within the context of a discrete Fourier transform, an additional complication arises: the autocorrelation of a bandpass filter will produce two spectral features corresponding to sum and difference frequencies, as illustrated in Fig. 4. In the case of a relatively narrow-band filter covering perhaps one eighth the alias width, the autocorrelation will consist of a feature near zero frequency and one at twice the central frequency of the bandpass filter. Comparison of Fig. 2 with Fig. 1 indicates that there is an additional feature at 3 times the central frequency, which is indicative of a third-order term. Broader band filters are illustrated in Figs. 5 and 6, covering one quarter and one half the alias bandwidth, respectively. As the filter bandpass is increased the high-frequency harmonic features cross the alias frequency and are folded back into the spectrum.

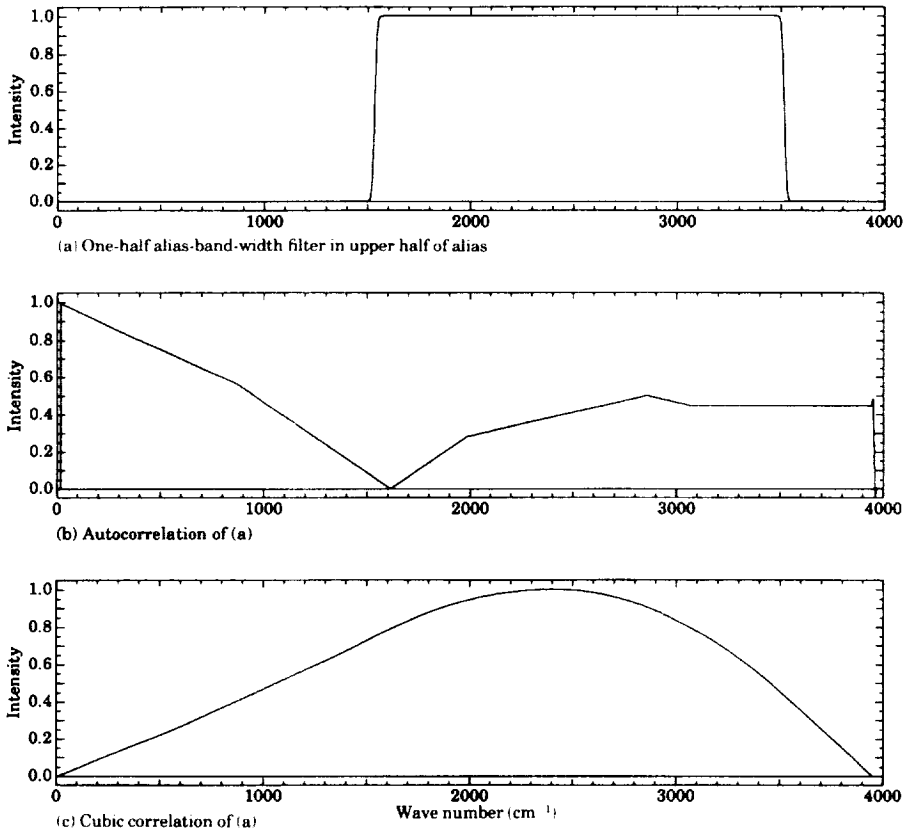

Fig. 6. (a) One-half alias-bandwidth model of ATMOS filter 3, (b) autocorrelation of (a), (c) cubic correlation of (a). The spectral artifact near zero frequency in (b) is distorted relative to that in Figs. 4 and 5, and the sum frequency artifact is largely aliased into the bandpass of the filter. Aliasing is evident in (b) and (c).

Implementation and Application

A nonlinearity correction must be applied to the raw interferogram before the initiation of the phase correction and Fourier transformation because the correction will alter the form of the interferogram immediately around the central fringe. The magnitude and location of the absolute maximum value may change and consequently alter the phase operator and hence the symmetry of the interferogram. Therefore the nonlinearity correction must be imple-

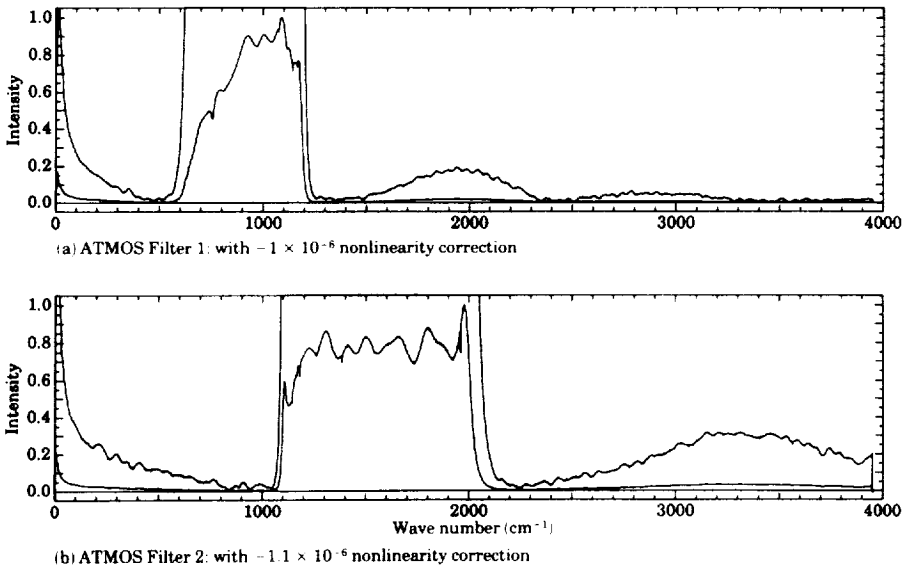

Fig. 7. ATMOS filters 1 and 2 high-Sun spectra after nonlinearity correction. Each frame contains two traces, one enlarged in the vertical by a factor of 10 to enhance the out-of-band spectral artifacts.

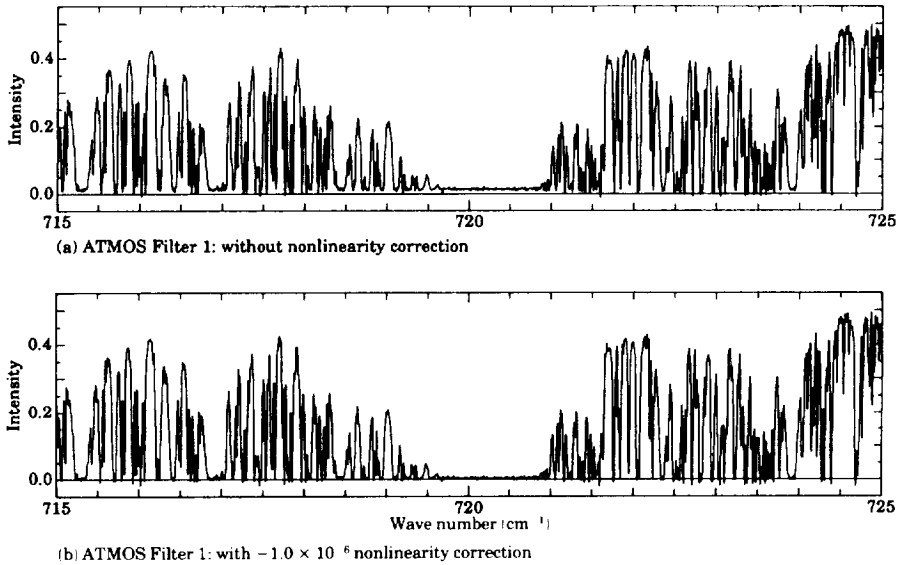

Fig. 8. ATMOS filter 1 low-Sun spectra: in-band comparison (a) before and (b) after nonlinearity correction.

mented before the phase evaluation and interferogram symmetrization to avoid biasing the phase spectrum with phase features resulting from the nonlinear harmonics of the actual spectrum.

In practice the estimation of the dc current level is an empirical process, in which a series of values are chosen and used in the nonlinearity correction before the Fourier-transformation process. Spectra with values of I_0 between 0.0 and -2.0×10^6 at increments of 1.0×10^5 are generated. A typical occultation event will include spectra throughout orbital sunset or sunrise with widely varying atmospheric air masses, ranging from 1.0×10^{-7} to 20.0×10^{-7} (tangent heights of 150 to 10 km), and consequently widely varying total flux levels and detector nonlinearity. Low-Sun spectra with a significant number of saturated atmospheric absorption features may have in-band offsets assessed in a straightforward manner, but high-Sun spectra can only be assessed in terms of the out-of-band artifacts. The resultant spectra are compared against the uncorrected spectra to evaluate the effectiveness of the parameter in changing the out-of-band artifacts and any in-band baseline offsets. A tradeoff between minimization of the out-of-band artifacts and in-band offsets is always necessary, and a compromise will have to be made. For the ATMOS instrument it is desirable to determine a set of nonlinearity-correction coefficients that produce an adequate correction for all flux levels. Figure 7 illustrates the out-of-band artifacts for ATMOS filters 1 and 2 with the optimal nonlinearity-correction coefficients and may be compared with Figs. 2(a) and 2(b). Figure 8 compares low-Sun spectra before and after correction in filter 1. Figure 8 suggests that within the bandpass of the filter, the principal effect of the proposed nonlinearity correction is the subtraction of a small constant, which could be accomplished in a much simpler fashion. However, spectra obtained at smaller air masses through the upper atmosphere do not have saturated spectral features. Under these conditions it would be impossible to estimate the necessary correction by inspection.

The case of ATMOS filter 3 is special, in that the spectral bandpass is almost one half the alias bandwidth of 3950 cm^{-1}. In such a case the nonlinear harmonic information at 2 and 3 times the central frequency of the filter is rejected by the antialiasing filter in the signal-processing electronics before the interferogram is sampled and recorded. The proposed model has the problem that it will introduce the harmonics and fold them back into the alias during the Fourier-transform process. With an adequate measurement of the antialiasing filter response it should be possible to refine the nonlinearity correction iteratively. Measurements of the filter response have proved insufficient because of the sample rate, which places the cutoff frequency at nearly 391.2 KHz, and circuit models of the filter, although plausible, did not provide enough information to permit successful iterative refinement of the nonlinearity-correction parameter. Other forms of nonlinear response were tried for filter 3. The coefficient of the cubic term, nominally 1/3, was adjusted to values between 0 and 1, without producing any clear improvement. We therefore concluded that the antialiasing filter was the major impediment to the correction of filter 3, not the assumed form of the response.

In the absence of a better model we have resorted to determining the residual baseline offset and subtracting it from the spectrum after phase correction and Fourier transformation. To remove both the slope remaining from the low-frequency artifact and the constant baseline offset remaining at high frequencies, two straight lines are fitted to the data in the out-of-band regions, and provided they intersect within the bandpass of the filter, these lines provide an adequate method for removing the baseline offsets within the filter bandpass. If the lines fail to inter-

sect then a constant baseline offset based on the high-frequency offset is all that can be applied. Typically this approach will bring the baseline offsets to within 1% of the zero level, although some care needs to be used to avoid negative baseline offsets under saturated spectral features.

Conclusions

A model of a nonlinear transfer function for removing spectral artifacts and offsets from Fourier-transform spectra obtained with single HgCdTe detector interferometers is proposed and evaluated. The method proves fully adequate for spectra that lie within the lower half of the spectral alias with bandpasses less than or equal to one half the alias bandwidth. When either or both of these conditions are violated, as occurs with certain optical filters, the correction method is insufficient to remove all the out-of-band spectral artifacts, and a post-transform baseline estimation and subtraction is used to remove the residual offsets.

In practice, theoretical approaches look promising, but the measured signal often seems to defy understanding, and empirical correction schemes look quite tempting. Two aspects complicate modeling of the nonlinear signal measured with a Fourier-transform spectrometer: the nonlinear distortion predominantly affects only a few points around the central fringe, and an accurate model of the electronic signal chain is essential for studying the effect of the detector nonlinearity alone. Application of a correction scheme to a filtered and sampled interferogram may or may not bear much relationship to the intended correction of the nonlinear distortion of the incident photon flux. Many years of spectroscopic evaluation of signal quality have gone into the development of the suggested correction scheme, and during that process the model has been generalized into a power series approach in pursuit of specific improvements. In the end none of the variations proved significantly better than the initial model.

This research was performed at the Jet Propulsion Laboratory (JPL), California Institute of Technology, under a contract with NASA. Much of this work is based in part on the work of the late R. H. Norton, who initially implemented and evaluated this method of nonlinearity correction for the ATMOS instrument. M. R. Gunson and R. Beer read preliminary versions of this manuscript and participated in many useful discussions about the method and its evaluation, and their assistance is gratefully acknowledged. We also thank E. Burgh, a summer student at the JPL in 1992, for testing our ideas on numerous examples. The technical support of J. C. Foster, J. S. Gieselman, and L. L. Lowes at the JPL is acknowledged and greatly appreciated.

References

1. F. Bartoli, R. Allen, L. Esterowitz, and M. Kruer, "Auger-limited carrier lifetimes in HgCdTe at high excess carrier concentrations," J. Appl. Phys. **45,** 2150–2154 (1974).
2. M. A. Kinch and S. R. Borrello, "0.1 eV HgCdTe photoconductors," Infrared Phys. **15,** 111–124 (1975).
3. S. R. Borrello, M. Kinch, and D. Lamont, "Photoconductive HgCdTe detector performance with background variations," Infrared Phys. **17,** 121–125 (1977).
4. R. A. Schindler, "Nonlinearity correction circuit for photoconductive detector," NASA Tech. Brief **10,** 47 (1986).
5. D. B. Chase, "Nonlinear detector response in FT-IR," Appl. Spectrosc. **38,** 491–494 (1984).
6. G. Guelachvili, "Distortion free interferograms in Fourier transform spectroscopy with nonlinear detectors," Appl. Opt. **25,** 4644–4648 (1986).
7. R. O. Carter III, N. E. Lindsay, and D. Beduhn, "A solution to baseline uncertainty due to MCT detector nonlinearity in FT-IR," Appl. Spectrosc. **44,** 1147–1151 (1990).
8. C. B. Farmer, "High resolution infrared spectroscopy of the Sun and the Earth's atmosphere from space," Mikrochim. Acta **3,** 189–214 (1987).